Jumps and concerted moves in Cu, Ag, and Au(110) adatom self-diffusion

F. Montalenti* and R. Ferrando†
INFM and CFSBT/CNR, Dipartimento di Fisica dell'Università di Genova, via Dodecaneso 33, 16146 Genova, Italy
(Received 12 October 1998)

We present a molecular-dynamics simulation of self-diffusion on the (110) surfaces of Cu, Ag, and Au. The metals are modeled by semiempirical potentials developed in the framework of the second-moment approximation to the tight-binding model. The energy barriers for the relevant diffusion processes are calculated by quenched molecular dynamics and compared with the available data in literature, obtaining a good agreement. The occurrence of long jumps is investigated in detail, showing that the three metals behave quite differently with this respect: long jumps are practically absent in Au and frequent in Cu. The effect of the specific features of the potential-energy surface and of the energy dissipation to the substrate on the probability of long jumps is investigated. The Arrhenius behavior of the jump rate is discussed, and deviations are found at high temperatures. Concerning correlated jump-exchange processes and double exchanges, we find that they are common in Cu even at rather low temperatures, whereas they are never observed in Au, Ag showing an intermediate behavior. [S0163-1829(99)01808-1]

I. INTRODUCTION

The study of isolated adatoms diffusion on metal surfaces is an important step in the understanding of many properties of technological interest, for example, in the fields of thin-film growth and catalysis.[1,2] Due to the development of different experimental techniques [mainly field ion microscopy (FIM) and scanning tunneling microscopy (STM)] it is possible to determine the microscopic mechanisms of diffusion. Many different diffusion mechanisms have been discovered. In fact, the diffusion of adatoms on metal surfaces may occur not only by uncorrelated hops between nearest-neighbor (NN) sites on the surface lattice, but also by exchanges (Ex) or by long jumps (in the following j_n will indicate an n-sites jump). In the exchange-mediated diffusion, the adatom enters the substrate and replaces one atom of the latter by pushing it above the surface; in the long-jump diffusion, the adatom starts from a given cell, then it makes a flight and finally stops in a cell that is not a nearest neighbor of the starting one.

The occurrence of exchange-mediated diffusion has been shown in many different systems.[2] A fast cross-channel diffusion on fcc(110) surfaces was discovered in Pt/Pt(110) and Ni/Ni(110) a long time ago.[3] Since cross-channel jump diffusion is not likely to happen (the adatom has to climb up a row), this strong mobility was first explained by a two-step mechanism: at a certain time, a vacancy is created in a row, and later the vacancy is filled by the original adatom. However, molecular-dynamics (MD) calculations[4] showed that the two-step mechanism would be energetically much less favorable than a concerted exchange process. Moreover, one has to assume that vacancies are created in the vicinity of the adatom, in order to have a reasonable probability of being filled in a short time. Later, the occurrence of the exchange process has been demonstrated experimentally in W/Ir(110).[5] Also on the more compact (100) surfaces, exchange diffusion is possible. This was already predicted on a bcc Lennard-Jones crystal surface by MD simulations,[6] and then it has been experimentally discovered on fcc surfaces of transition metals, such as Pt and Ir,[7] that exchange is the dominant diffusion mechanism. Recently, MD simulations on the (100) faces of Cu (Refs. 8 and 9) and other metals[10] have shown that complicated exchange mechanisms, involving the concerted motion of many atoms, become important at high temperatures.

The occurrence of long jumps (often called correlated jumps) has been demonstrated experimentally in different systems,[11–14] such as Ir/W(110), Na/Cu(001), Pd/W(211), and Pt on missing-row reconstructed Pt(110). The possibility of long jumps has also been investigated from the point of view of the theory;[15–23] such events have also been found in many molecular-dynamics simulations (see, for example, Refs. 9,24–30). However, we remark that it is not easy to extract general trends from experimental data for what concerns the occurrence of long jumps. In fact, similar systems behave in very different ways. For example, in FIM experiments on metal adatom diffusion on a channeled surface like W(211), the following results were found:[11,13] in the case of Re and Mo there was no evidence of long jumps near room temperature; for Ir and Rh few ($\sim$3%) long jumps were found; and finally, in the case of Pd there was a significant fraction ($\sim$20%) of long jumps already well below room temperature.

In this paper we study the diffusion of adatoms on the (110) surfaces (see Fig. 1) of Cu, Ag, and Au by MD simulations, up to temperatures of the order of half of the melting temperature T_M. We shall focus our attention on all the above-mentioned correlated diffusion processes. In the case of Au we consider only the (1×1) geometry, which is easily compared to the corresponding surfaces of Cu and Ag, the latter metals being more stable in the (1×1) geometry. The $(110)(1\times2)$ surface of Au, which is the most stable for that metal, has been studied elsewhere.[31]

Cu, Ag, and Au are modeled by tight-binding many-body potentials as developed by Rosato, Guillopè, and Legrand (RGL).[32,33] The RGL potentials reproduce the surface reconstructions of noble metals.[33] They have been widely used in the simulation of diffusion on transition- and noble-metal

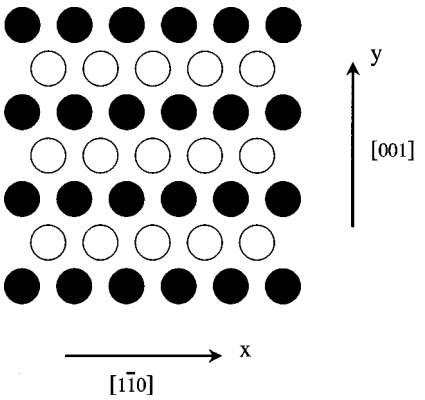

FIG. 1. The (110) surface geometry. The solid dots are the top-row atoms and the open circles are the atoms of the layer just below.

surfaces,[9,29,34] where they predict the dominant diffusion mechanisms, in agreement with the experimental results.[35] On the (110) surfaces of the noble metals, diffusion proceeds by jumps in the in-channel $[1\bar{1}0]$ direction and by exchanges in the cross-channel [001] direction, the cross-channel jump requiring a very high activation barrier.[29,36,37] At high temperatures, long jumps and other correlated exchange mechanisms (CEx), such as jump exchanges, double exchanges, and others, may appear. This has been shown in a MD simulation of Ag(110),[29] and here we investigate if these mechanisms are common to the nonreconstructed (110) surfaces of other metals, like Cu and Au. As can be seen in the following, Cu, Ag, and Au present different behaviors. Correlated jump-exchange events are frequent even at rather low temperatures in Cu, are possible in Ag only above ~ 550 K, and are practically absent in Au. Also, long jumps are much frequent in Cu than in Ag and practically absent in Au.

The paper is organized as follows. Section II contains the description of the RGL potentials. Section III contains the results concerning the static energy barriers for the different diffusion mechanism; here we make a rather comprehensive test of the reliability of RGL potentials comparing their results with those obtained by other semiempirical potentials, by *ab initio* calculations, and by experiments. We consider also the (100) surface because there both *ab initio* results and experimental data are available. Section IV contains the results of the high-temperature simulations of adatom diffusion on the unreconstructed (110) surfaces of Cu, Ag, and Au, and Sec. VI contains the conclusions.

II. MODEL

As is well known, metals cannot be realistically modeled by means of pair potentials, such as Lennard-Jones or Morse,[38,39] and it is necessary to employ many-body potentials. Because of this, many different semiempirical potentials have been proposed for transition and noble metals: effective-medium theory,[40] the glue model,[41] embedded-atom,[42] Sutton-Chen,[43] and RGL potentials. The latter will be employed in the following calculations. By the semiempirical potentials, it is possible to give a reasonably accurate description of the metals with a computational effort of the same order of magnitude of the one required by pair potentials. In this way, simulations with thousands of atoms on time scales up to hundredths of nanoseconds are feasible. However, since those potentials are built on rather crude approximations of the electronic structure of the metals, their reliability must always be checked against experiments and *ab initio* calculations.

The many-body RGL potential has been developed in the framework of the second-moment approximation (SMA) of the density of states in the tight-binding model.[32,38,44–46] In the SMA, the band energy E_b^i for a given atom i is proportional to the square root of the second moment of the local density of states; the latter is written as a sum of square hopping integrals (with an exponential dependence on the interatomic distance) between the neighbors. For a derivation of the SMA for noble metals see Ref. 47 (the usual derivation better applies for the transition metals, whose d band is not completely filled). The band energy gives an attractive many-body term; the stability of the crystal is insured by adding a phenomenological core-repulsion term E_r^i of the Born-Mayer type. Thus, the total energy of atom i is the sum of E_b^i and E_r^i. E_b^i reads:

$$E_b^i = -\left\{ \sum_{j, r_{ij} < r_c} \xi^2 \exp\left[-2q\left(\frac{r_{ij}}{r_0} - 1 \right) \right] \right\}^{1/2}, \qquad (1)$$

where ξ is an effective hopping integral, r_{ij} is the distance between the atoms i and j, r_c is the cutoff radius for the interaction, r_0 is the first-neighbor distance (2.89 Å in Ag, 2.88 Å in Au, and 2.56 Å in Cu), and q gives the distance dependence of the hopping integral. E_r^i is written as

$$E_r^i = \sum_{j, r_{ij} < r_c} A \exp\left[-p\left(\frac{r_{ij}}{r_0} - 1 \right) \right]. \qquad (2)$$

The cohesive energy of the crystal is then

$$E_c = \sum_i (E_b^i + E_r^i). \qquad (3)$$

The parameters (ξ, A, p, q) are fitted to the experimental values of the cohesive energy, the lattice parameter, the bulk modulus, and the elastic constants C_{44} and C'. The cutoff r_c is taken as the second-neighbor distance. The values used in the following are $p = 10.55$, $q = 2.43$, $A = 0.089\,38$ eV, $\xi = 1.280$ eV for Cu; $p = 10.85$, $q = 3.18$, $A = 0.10\,31$ eV, $\xi = 1.190$ eV for Ag; and $p = 10.53$, $q = 4.30$, $A = 0.21\,97$ eV, $\xi = 1.855$ eV for Au.

III. CALCULATION OF THE STATIC ENERGY BARRIERS

The static energy barriers for the different diffusion processes are obtained by quenched molecular dynamics.[48] A detailed account of our procedure is found in Refs. 28 and 49.

In order to test the quantitative accuracy of the diffusion barriers for Ag and Cu, as calculated by RGL potentials, we compare our values with those obtained by experiments, *ab initio* calculations, and other semiempirical methods on the (100) and (110) surfaces of these metals. Unfortunately, on

TABLE I. Diffusion barriers on (100) surfaces.

Process	RGL	EM	CEM	EA(VC)	EA(AFW)	LDA	GGA	Experiment
Cu jump	0.39	0.40[a]	0.47[c]	0.53[d]	0.38[d]	0.65-0.75[g]	0.51-0.55[g]	0.39±0.06[j] 0.36±0.03[k] 0.40[l] 0.28±0.06[m]
Cu exchange	0.79		0.43[c]	0.79[d]	0.72[d]	1.03-1.23[g]	0.82-0.96[g]	
Ag jump	0.43	0.37[a]	0.41[c]	0.48[d]	0.48[d]	0.52[h]	0.45[h]	0.40±0.05[n] 0.38[o]
Ag exchange	0.61	0.61[a]	0.58[c]	0.60[d]	0.75[d]	0.93[h]	0.73[h]	
Au jump	0.51	0.49[b]		0.84[d]	0.64[d]	0.83[i]	0.58[i]	
Au exchange	0.41			0.32[d]	0.30[d]	0.65[i]	0.40[i]	
Cu along steps	0.26	0.26[a]			0.25[f]			
Ag along steps	0.25	0.22[a]		0.26[e]		0.30[h]	0.27[h]	
Au along steps	0.32	0.30[b]						
Cu jump descent	0.71	0.58[a]			0.77[f]			
Cu exchange descent	0.52	0.63[a]			0.51[f]			
Ag jump descent	0.59	0.48[a]				0.70[h]	0.55[h]	
Ag exchange descent	0.55	0.52[a]				0.52[h]	0.45[h]	
Au jump descent	0.57	0.55[b]						
Au exchange descent	0.51	0.53[b]						

[a]From Merikoski *et al.* (Ref. 51).
[b]From Stolze (Ref. 52).
[c]From Perkins and DePristo (Ref. 53).
[d] From Liu *et al.* (Ref. 36).
[e]From Nelson *et al.* (Ref. 54).
[f]From Karimi *et al.* (Ref. 55).
[g]From Boisvert and Lewis (Ref. 56).
[h]From Yu and Scheffler (Ref. 57).
[i]From Yu and Scheffler (Ref. 58).
[j]From Breeman and Boerma (Ref. 59).
[k] From Durr *et al.* (Ref. 60).
[l]From De Miguel *et al.* (Ref. 61).
[m]From Ernst *et al.* (Ref. 62).
[n]From Langelaar *et al.* (Ref. 63).
[o]From Bardotti *et al.* (Ref. 64).

the (110) surface, experimental results are available only for Au,[50] while for the other two metals only calculations by semiempirical potentials are found in the literature. Because of this, we test the reliability of our calculations also on the (100) surfaces of the three metals, because there either experimental results or *ab initio* calculations have already been performed. The results are summarized in Table I [(100) symmetry] and Table II [(110) symmetry].

In the case of the (100) surfaces, we consider the following processes: (a) diffusion of an adatom on the flat surface, both by *jump* via bridge site and by *exchange*; (b) diffusion of an adatom along a straight high-symmetry step; and (c) descent of an adatom from a terrace limited by a straight high-symmetry step, both by *jump* and by *exchange*.

RGL results are compared to effective medium (EM),[51,52] corrected effective medium (CEM),[53] embedded atom [in the Voter-Chen parametrization, EA(VC) (Refs. 36 and 54) and in the Adams-Foiles-Wolfer parametrization, EA(AFW) (Refs. 36 and 55)], *ab initio* density-functional calculations in the local-density approximation (LDA),[56–58] *ab initio* density-functional results with gradient corrections (GGA) (Refs. 56–58), and experimental results.[59–64] For process (a), RGL potentials predict that jump is favored over exchange in Ag and Cu, whereas in Au the opposite happens. This agrees

TABLE II. Diffusion barriers on (110) surfaces.

Process	RGL	EM	CEM, MD-MC/CEM	EA (AFW)	EA (VC)	Experiment
Cu in channel	0.23	0.29[a],0.18[b]	0.08,0.26[c]	0.24[d]	0.53[d]	
Cu cross channel	0.29	0.56[a],0.26[b]	0.09,0.49[c]	0.30[d]	0.31[d]	
Ag in channel	0.28	0.29[a]	0.26,0.25[c]	0.32[d]	0.25[d]	
Ag cross channel	0.38	0.56[a]	0.34,0.33[c]	0.42[d]	0.31[d]	
Au(1×1) in channel	0.28	0.27[a]		0.34[d],0.27[d]	0.25[d]	>0.38[f]
Au(1×1) cross channel	0.46	0.55[a]		0.42[d],0.35[e]	0.40[d]	
Au(1×2) in channel	0.31					0.40-0.44[f]

[a]From Stolze (Ref. 52).
[b]From Hansen *et al.* (Ref. 66).
[c]From Perkins and DePriste (Ref. 37).
[d]From Liu *et al.* (Ref. 36).
[e]From Roelofs *et al.*, (Ref. 65).
[f]From Gunther *et al.* (Ref. 50).

well with all *ab initio* results and with both EA calculations, while CEM predicts that exchange is favored also in Cu. The experimental data in Cu and Ag are in very good quantitative agreement with the RGL values for the jump mechanism (except for the last experimental value in Cu, which gives a much lower barrier). We notice that the experiments do not determine the diffusion mechanism, but since most calculations indicate that in Ag and Cu jump diffusion should prevail, there is a strong indication that the measured barrier is the one for jump diffusion. For process (b), all available calculations give results in good agreement with each other in any of the three metals. For process (c), RGL calculations predict that exchange descent should always prevail. This agrees with the *ab initio* results in Ag and with the EA(AFW) calculations in Cu. On the contrary, the EM results predict jump descent in both Ag and Cu (however the energy difference between the two mechanisms are rather small).

In the case of the (110) surface (see Table II), experimental results (by STM[50]) are available only in the case of Au, both in the (1×1) and (1×2) geometries. In this case, RGL potentials correctly predict a slightly higher diffusion barrier (by about 10%) for the (1×2) with respect to the (1×1). However, the absolute values of the barriers are smaller than in experiments. On the other hand, all the calculations by semiempirical potentials underestimate the barrier for diffusion on the (1×1),[36,65] the lowest and the highest results being given by EA(VC) and by EA(AFW) calculations, respectively.[36] A detailed comparison in the case of Cu and Ag can be done only with other calculations. We consider EM,[52,66] CEM and MD-MC/CEM,[37] EA(AFW),[36] and EA(VC) (Ref. 36) results, for in-channel jump diffusion and cross-channel exchange diffusion—the cross-channel jump being very unlikely since it requires a very large activation energy. In Ag, the available data are all in good agreement with each other, except for the EM estimation of the exchange cross-channel diffusion barrier in Ag. In Cu, the RGL results for in-channel jump diffusion are in reasonable agreement with the EM, MD-MC/CEM, and EA(AFW) data, whereas the CEM and the EA(VC) calculations give a much lower and much higher barrier, respectively. For cross-channel exchange diffusion, RGL results are in good agreement with EA(AFW), EA(VC), and one of the two EM calculations. In this case, the other potentials give either very low or very high barriers.

The above-illustrated comparisons show that on the (100) surfaces RGL potentials predict the diffusion mechanism in agreement with the available *ab initio* calculations, and, where the comparison with experimental data is possible, the quantitative agreement is very good. On the (110) surface, the comparison with experimental data in Au shows a qualitatively correct difference between the (1×1) and (1×2) geometries, but the absolute values of the energies are lower by $\sim25\%$ than those measured in the experiment. On the other hand, the comparison with the existing literature is very favorable in Ag, while in Cu there is still some debate. We remark however that in Cu(110) RGL potentials agree with the majority of the existing data and that the data in disagreement predict both very high and very low barriers.

IV. HIGH-TEMPERATURE DIFFUSION ON THE (110) SURFACES

Extensive high-temperature simulations of the diffusion on the (110) surface of the three metals have been performed. In the case of Cu eight different temperatures between 300 and 600 K have been considered. The highest temperature is well below the temperature at which a significant disordering of the surface occurs.[67] In the case of Ag, data have been taken at 450, 550, and 600 K, whereas for Au we simulated only at 450 K because at higher temperatures the unreconstructed surfaces disorder quickly. In our simulations, Newton's equations of motion have been solved by the Verlet algorithm,[68] with time steps in the range 3.5–7 fs. With these time steps, energy is always conserved to better than one part over 10^5. The simulations have been performed on a (7×8) slab with a thickness of 15 layers and with two adatoms (one on each surface of the slab). Periodic boundary conditions have been imposed on the surface plane. All atoms in the slab have been left free to move. Thermal expansion has been taken into account as explained in Ref. 28.

The high-temperature simulations have displayed a rich phenomenology with different kinds of events. We may classify events into three main groups: in-channel jumps, cross-channel exchanges, and correlated jump-exchange (or exchange-exchange) events. The Secs. IV A–IV C are devoted to the study of these different kinds of events.

A. In-channel mobility: Arrhenius behavior of the jump rate

In-channel mobility may take place by single and long jumps. First, we analyze the temperature dependence of the total jump rate r_j in Cu. We have chosen Cu because in this metal it is easier to accumulate statistics down to room temperature, due to the smaller in-channel diffusion barrier. r_j is obtained at each T dividing the total number of jumps (see the lines j_1 and j_2 in Table III) by the total simulation time. Usually it is assumed that the T dependence of r_j should follow the Arrhenius law,

$$r_j = r_j^0 \exp\left(-\frac{\Delta E_j}{k_B T}\right), \tag{4}$$

where r_j^0 is the prefactor and ΔE_j is the activation (or dynamic) barrier. In the standard form of the Arrhenius law, which is usually employed for example in fitting the experimental data, both the prefactor and the activation barrier are assumed as T independent. In real systems, however, there may be deviations from the Arrhenius law, and those deviations are often accounted for by introducing a T dependence of the prefactor and of the barrier. Recent literature shows that a correct way to take into account such deviations is still under debate. Indeed, theoretical calculations on Ag,[69,70] Cu,[69,70] and Ni[70] self-diffusion on the (100) surface, in the framework of transition state theory and of the quasiharmonic approximation to the lattice dynamics, suggested that the activation barrier for jump diffusion should decrease with T. In particular, at 600 K such barrier should be almost 10% lower when compared to the static one. Boisvert *et al.*

TABLE III. Cu self-diffusion on the (110) surface: summary of the events. Few multiple jumps have been observed also, but they are not reported. Usually, correlated events are in majority jump exchanges (je) or exchange jumps (ej) (more or less in the same proportion), with fewer double exchanges (ee) and very few more complicated processes (such as jump exchange jump etc.). For instance at 600 K we find 19 ej, 14 je, and 6 ee.

T(K)	300	315	350	400	450	500	550	600
Simulation time (ns)	72	45	135	40.3	18.3	7.9	4	3.9
j_1	158	145	971	669	512	335	264	260
j_2	2	5	26	42	37	40	35	41
j_2 (%)	1	3	3	6	7	11	12	14
Ex	17	14	116	100	109	79	68	73
CEx	0	0	13	16	17	26	22	39
CEx (%)	0	0	10	14	13	25	24	35

argued[71] that it is true that the energy barrier depends on T, but linearly so that the effect only causes a prefactor renormalization and no real temperature dependence of the activation barrier is present. The same authors explicitly showed,[72] by MD simulations of Cu/Cu(100) diffusion, that considering a wide range of T (from 100 to 800 K), no appreciable deviation from the Arrhenius law is found. Apart from the above-mentioned (possible) corrections to Eq. (4) due to the lattice dynamics influence on diffusion, ''finite-barrier'' effects should also be taken into account. We recall that Eq. (4) is only asymptotically valid in the limit $\Delta E_j/k_BT \to \infty$. In particular, it has been shown[16,78] that when the ratio between the static energy barrier and k_BT is smaller than ~ 5 deviations from the Arrhenius law should be expected. We remark that the way the finite-barrier effects modify the Arrhenius behavior can be quite different from system to system, since they are related to the anharmonic part of the force felt by the adatom. In all the above-mentioned references[69–72] the finite-barrier effects should be negligible up to ~ 1000 K due to the high static diffusion barriers (of the order of 0.5 eV).

Here we study this problem in the case of Cu/Cu(110) considering many different temperatures in a wide range (from 300 to 600 K); at each T we accumulate a rich statistics of events (again see Table III). In Fig. 2 we report the Arrhenius plot of r_j in the above-T range and we estimate ΔE_j and r_j in three different ways in order to discuss their actual temperature dependence. First, we have fitted the Arrhenius law [Eq. (4)] in the whole temperature range, obtaining $\Delta E_j = 0.186 \pm 0.003$ eV and $r_j^0 = 4$ ps^{-1}. In this way, ΔE_j turns out to be significantly smaller than the static energy barrier (the latter being of 0.23 eV). However, as can be seen in Fig. 2, the fitting is rather poor, because the points at the lowest and the highest temperatures do not accommodate well on the straight dashed line. Both facts (ΔE_j being smaller than the static barrier and a bad fit of some points) indicate that there is some deviation from the standard Arrhenius behavior at high T.[74–77] Following this indication, we have made two further fits: in one we take into account only the four low-T points (up to 400 K), and another with the high-T points. The low-T fit is practically perfect; it gives $\Delta E_j = 0.213 \pm 0.007$ eV and $r_j^0 = 9$ ps^{-1}. In this case the dynamic barrier is very close to the static one (within three standard deviations), indicating that, up to 400 K, there is no clear evidence of deviations from the standard Arrhenius behavior. On the contrary, at high T we obtain a much lower $\Delta E_j = 0.16 \pm 0.01$ eV and a smaller prefactor ($r_j^0 = 2$ ps^{-1}). This result is in qualitative agreement with one-dimensional Langevin approaches,[16,78] where it was shown that the finite-barrier effects cause a lowering of both prefactor and barrier at high temperatures. [Note that for the system considered here $E_j/(k_BT) \sim 5$ if $T \sim 500$ K]. We emphasize that lattice-dynamics effects could give their contribution to the barrier lowering as well, but presently we are not able to separate their contribution from the one given by the finite-barrier corrections. Our results are in qualitative agreement with those of the simulations in Ref. 73, even if a direct quantitative comparison is not possible due to the lack of any information on the statistics of the results in Ref. 73.

It is worth mentioning that if instead of the jump rate we consider the in-channel diffusion coefficient D, which in a jump-theory framework is given by

$$D = \frac{1}{2} a^2 r_j \sum_l l^2 p_l \tag{5}$$

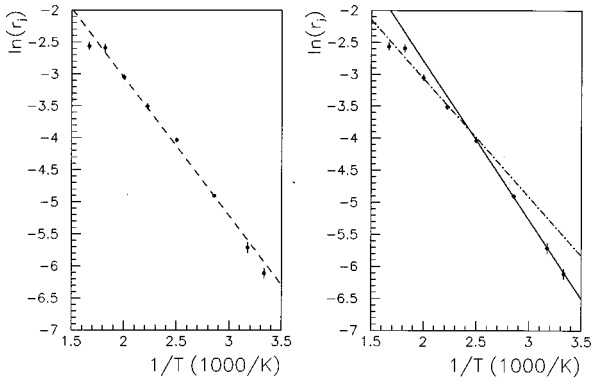

FIG. 2. Arrhenius plot of r_j in Cu. r_j is in ps^{-1}. Left panel: the dots correspond to the simulation results, and the line to the best fit of the Arrhenius law in the whole temperature range. This fit is poor, since the high-T and the low-T points do not accommodate well on the line. Right panel: here the simulation results are separately fitted in the low-T range (solid line) and in the high-T range (dash-dotted line). The low-T fit is practically perfect up to 400 K (the four points at right), and its slope is close to the static energy barrier.

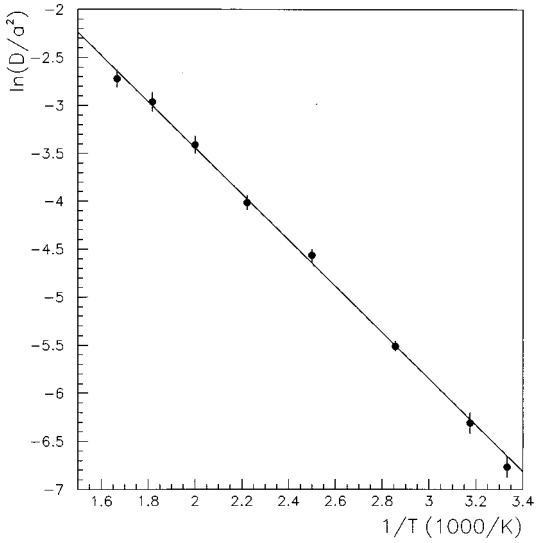

FIG. 3. Arrhenius plot of the in-channel diffusion coefficient D (divided by the square of the unit-cell length a) for Cu/Cu(110) self-diffusion. D/a^2 is in ps^{-1}. Due to the compensation coming from the long-jumps contribution, points now well accommodate on a straight line.

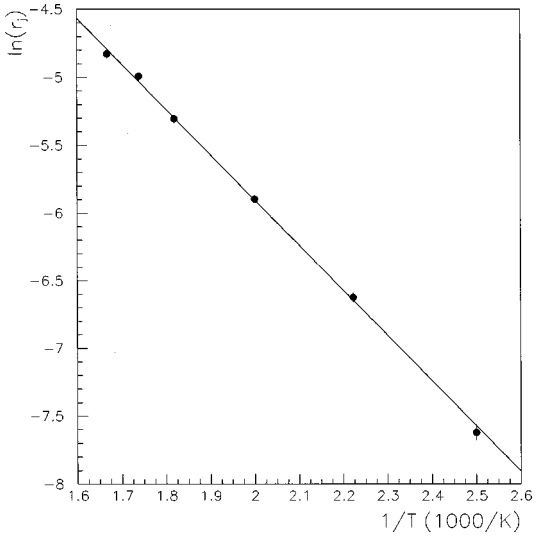

FIG. 4. Arrhenius plot of r_j for Au/Au(110)(1×2) self-diffusion (data taken from Ref. 31). r_j is in ps^{-1}. The points well accommodate on a straight line, whose slope is close to the static energy barrier.

(p_l is the probability to have an l-sites jump, and a is the distance between adjacent in-channel minima), the long-jumps contribution acts in such a way to restore the Arrhenius behavior at high temperatures, since the long-jumps rate raises with temperature (see Sec. IV B). Indeed, this can be easily seen in Fig. 3, where the linear fit turns out to be much closer to the MD points (compare the fit in the left panel of Fig. 2). Moreover, if we estimate the slope of such straight lines, we obtain an effective barrier of 0.21 ± 0.01 eV, which is within two standard deviations from the static barrier.

Summarizing, it arises clearly from our results that, if T is low enough for the finite-barrier effects to be neglected, the Arrhenius law is very well satisfied, and the corresponding barrier is (within 5%) the static one. These considerations are validated by our results on Au/Au(110)(1×2) diffusion presented in Ref. 31, from which we extract here the Arrhenius plot of the jump rate (see Fig. 4). For this system the static barrier is 0.31 eV, and thus in the whole temperature range of the simulations (from 350 to 625 K) small finite-barrier effects are expected (in fact, the dynamic barrier is 0.288 ± 0.005 eV, which is close to the static one).

B. In-channel diffusion: single and long jumps in Cu, Ag, and Au

Now we focus our attention on a comparison between in-channel diffusion for the three metals. It turns out that the static energy barrier for in-channel diffusion is essentially the same in Au and Ag, and somewhat lower in Cu (see the first column of Table II). From these data one could expect that the behavior of adatoms diffusing on those metals would be similar, and the only difference would be that diffusion of Cu on Cu is activated at lower temperatures. On the contrary the high-temperature simulations show rather different behaviors, especially for what concerns the occurrence of long jumps. From Table IV it turns out that, at 450 K, long jumps are practically absent in Au, about 3% of the total jumps in Ag and about of 6% in Cu. In the latter metal, at 600 K, nearly 15% of long jumps are found, a percentage which is never reached in Ag at any temperature.[29] In the following we show that these differences can be understood in terms of two factors: the energy dissipation rate of the adatom on the easiest diffusion path and the multidimensional topology of the potential energy surface. As we show in the following, both factors are favorable for Cu and the contrary happens for Au.

TABLE IV. Single jumps (j_1), double jumps (j_2), exchange cross-channel (Ex), and correlated exchange cross-channel (CEx) statistics. j_2 (%) is calculated over the total number of in-channel jumps, CEx (%) on the total number of cross-channel events. Few multiple jumps have been found also, but they are not reported.

	Ag	Au	Cu	Ag	Cu	Ag	Cu
T (K)	450	450	450	550	550	600	600
Simulation time (ns)	30	94.5	18.3	10.1	4.0	4.4	3.9
j_1	210	280	540	209	264	142	260
j_2	6	2	37	8	35	13	41
j_2 (%)	2.8	0.7	6.4	3.7	11.7	8.4	13.6
Ex	36	15	115	46	64	35	73
CEx	1	0	17	5	22	9	39
CEx (%)	2.7	0	13	9.8	26	20	35

Let us consider the energy dissipation on the easiest diffusion path. In all metals, the z coordinates of the minima and of the saddle points essentially coincide, and therefore the easiest diffusion path is a straight line along the x direction in the middle of the channel. Therefore, the differences between the metals are not due to nonrectilinear diffusion paths, as it happens in other cases.[28,79] By restricting our considerations to the easiest diffusion path we reduce our problem to the diffusion in a one-dimensional periodic potential. If we assume that the adatom is coupled to the substrate with a friction η per unit mass and with a δ-correlated noise,[81] it can be shown that the probability of long jumps depends on the dissipation parameter Δ (see Ref. 17), defined as follows:

$$\Delta = \frac{\eta}{k_B T}\int_0^a \sqrt{2m[U_s - U(x)]}\,dx, \tag{6}$$

where a is the lattice spacing along the $[1\bar{1}0]$ direction, U_s is the potential energy at the saddle point, and $U(x)$ is the potential energy along the easiest diffusion path. In all metals $U(x)$ is well approximated by a cosine; if E_b is the static energy barrier for in-channel diffusion, and $k_B T \ll E_b$, the following expression for Δ is obtained:

$$\Delta \simeq \frac{2\eta a}{\pi k_B T}\sqrt{2mE_b}. \tag{7}$$

The friction can be estimated by the decay time of the mass-normalized velocity autocorrelation function $Z(t)$ along the x direction

$$Z(t) = \tfrac{1}{2} m\langle v_x(t) v_x(0)\rangle. \tag{8}$$

If the potential well is sufficiently deep, $Z(t)$ is well approximated by its expression for a harmonic well, which turns out to be[82]

$$Z(t) = A\ \exp(-\eta t/2)\cos(\omega t) \tag{9}$$

with $Z(0) = A = k_B T/2$. Let us consider $T = 450$ K, a temperature at which the expression (9) fits well the actual behavior of $Z(t)$ as obtained from the simulations for all three metals. For example, at that temperature we obtain $\eta = 1.5\ \text{ps}^{-1}$ in Au. This value is compatible with the one found by Roelofs *et al.*[80] at 400 K, which is $\eta = 2.6\ \text{ps}^{-1}$ (the latter value is determined with an accuracy of about a factor of 2, as explained in Ref. 80).

Since the $Z(t)$ shows several oscillations in Cu and Ag and fewer in Au (see Fig. 5), we can expect that dissipation would be larger in Au than in the other metals. This is the case: by fitting the curves shown in Fig. 5 by a $Z(t)$ of the form (9), and using Eq. (7), one finds that Δ is of the order of 10 in all three metals (corresponding to a few percent of long jumps[15]) but $\Delta_{\text{Cu}}/\Delta_{\text{Ag}} \simeq 1.1$ and $\Delta_{\text{Cu}}/\Delta_{\text{Au}} \simeq 0.8$. These results indicate that in gold fewer long jumps should be found, in agreement with the results of the simulations, but they do not explain the large difference (of one order of magnitude) in the percentages between Au and Cu (see Table IV). Therefore, the one-dimensional model of diffusion along the most favorable diffusion path, even if it is in some qualitative agreement with the results of the simulations, is not sufficient. In fact, the explanation of these differences must take also into account the multi-dimensional topology of the adiabatic potential[83] felt by the adatom.

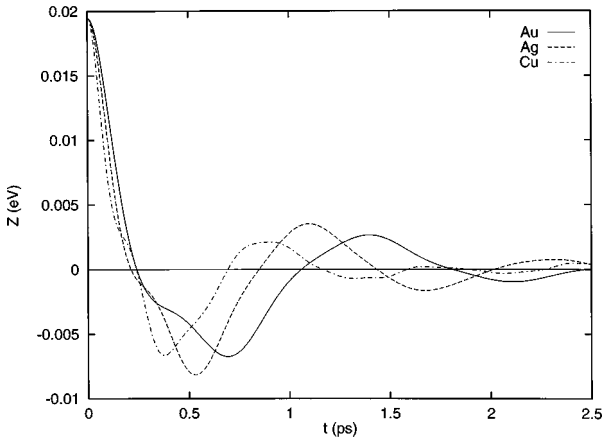

FIG. 5. The velocity autocorrelation function $Z(t)$ [see Eq. (8)] for the three metals. The dash-dotted, dashed, and solid lines correspond to Cu, Ag, and Au, respectively.

In order to understand this topology, we have calculated two different potential-energy surfaces by quenched MD. First, we have fixed the x and y coordinates of the adatom within a lattice cell, letting then its z coordinate and all the degrees of freedom of the substrate free to relax. In this way we obtain a two-dimensional (2D) potential $V(x,y)$ [see Fig. 6, where $V(x,y)$ is shown for Cu]. From $V(x,y)$ one may recover the curvatures around the minima and the saddle points. Around the minimum, the curvatures are proportional to the squares of the frequencies $(\omega_m^{xx}, \omega_m^{yy})$; around the saddle point, the x degrees of freedom is unstable and the corresponding frequency is imaginary $(i\omega_s^{xx}, \omega_s^{yy})$. According to the multidimensional extension of Kramers theory of activated process,[84] the prefactor in r_j is proportional to the ratio

$$f = \omega_m^{yy}/\omega_s^{yy}. \tag{10}$$

This means that the jump rate is larger when the potential-energy surface is wider at the saddle point than at the mini-

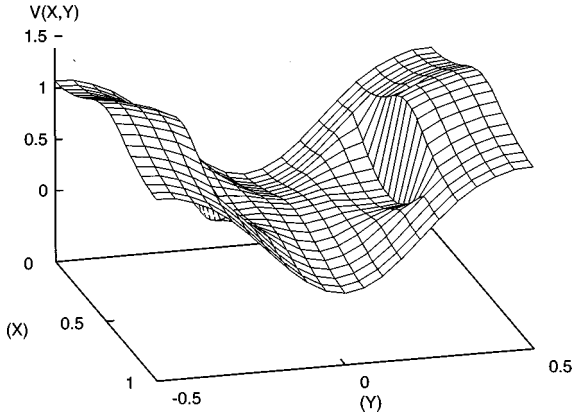

FIG. 6. Potential-energy surface $V(x,y)$ for Cu self-diffusion. $V(x,y)$ is obtained fixing the x and y coordinates of the adatom and letting all other degrees of freedom in the system relax.

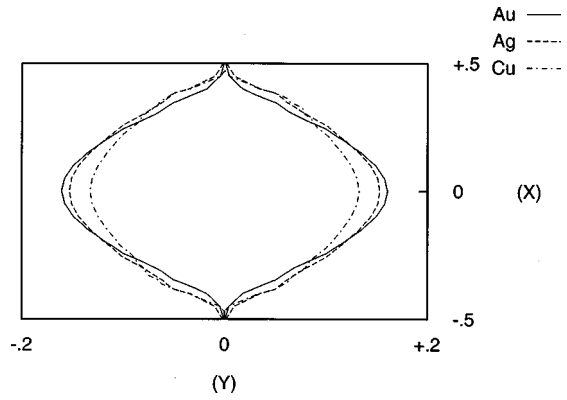

FIG. 7. Contour plot of $V(x,y)$ at the saddle-point energy E_s. The dash-dotted, dashed, and solid lines correspond to Cu, Ag, and Au, respectively.

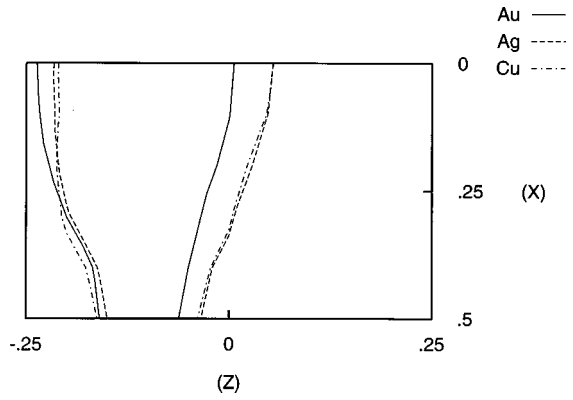

FIG. 9. Contour plot of $V(x,z)$ at the energy $E_h(T)=E_s+k_BT$, with $T=450$ K. The dash-dotted, dashed, and solid lines correspond to Cu, Ag, and Au, respectively.

mum ($\omega_m^{yy}>\omega_s^{yy}$). Moreover, it has been shown, in model-potential calculations of diffusion in periodic systems,[85] that the fraction of long jumps increases significantly with f. In our case we obtain $f_{\mathrm{Au}}=0.92$, $f_{\mathrm{Ag}}=0.99$, and $f_{\mathrm{Cu}}=1.11$. This indicates again that Au is less favored for long jumps, and the contrary happens for Cu.

Another way of looking at the effect of the topology of the potential on long jumps is to consider the contour plots of $V(x,y)$. In Figs. 7 and 8 we report the contour plots of $V(x,y)$ at the saddle-point energy $E_h(0)=E_s$ and at $E_h(T)=E_s+k_BT$, with $T=450$ K, respectively. $E_h(T)$ is the average energy of the particles hopping out from a well at a given T.[86] It is evident that Au presents the widest contour plot at the minimum position and the narrowest at the saddle point, while for Cu the opposite happens. In fact, from Fig. 8, it turns out that the ratio between the width at the saddle point and at the minimum is 0.48 for Cu, 0.32 for Ag, and 0.28 for Au.

Then, in order to also check the vertical motion of the adatom, we have repeated the above procedure but fixing the x and z coordinates of the adatoms, thus obtaining a potential $V(x,z)$. Again, the contour plots at $E_h(T)$, with $T=450$ K (see Fig. 9), show that Au has the narrowest saddle point and Cu the largest. In this case, the ratio of the widths is 0.48 for Cu, 0.44 for Ag, and 0.40 for Au. In conclusion, Au presents the most unfavorable potential topology for long jumps and Cu the most favorable. This, together with the somewhat higher dissipation, qualitatively explains why long jumps are very few in Au. In Cu, the better topology overcompensates for the slightly larger dissipation with respect to Ag.

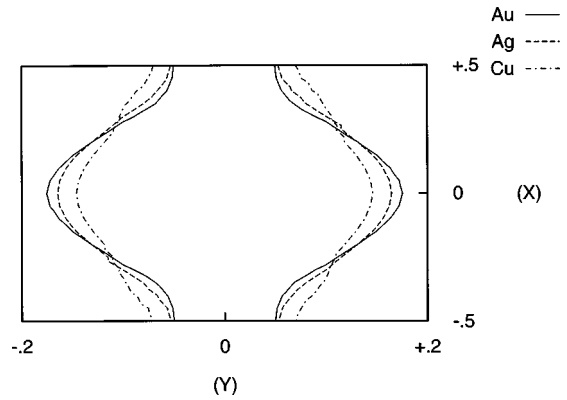

FIG. 8. Contour plot of $V(x,y)$ at the energy $E_h(T)=E_s+k_BT$, with $T=450$ K. The dash-dotted, dashed, and solid lines correspond to Cu, Ag, and Au, respectively.

Another interesting point concerning the fraction of long jumps is its dependence on T. By FIM, it has been found in Pd/W(211) (Ref. 13) that the percentage of long jumps increases from practically 0 to 20 % in a very narrow temperature range (from 122 to 133 K); on the other hand, in STM experiments on Pt/Pt(110) (1×2) (Ref. 14) the fraction of long jumps increases with T, but not in such a dramatic way. MD simulations in different systems[9,28,29] have shown that the fraction of long jumps clearly increases with T but not with changes of orders of magnitude in ranges of 10 K. From the point of view of the theory, the 1D Langevin model with T-independent friction[15,19] gives an even milder increase of the fraction of long jumps. Very recent results based on a kinetic theory developed in the framework of the Boltzmann equation[23] suggest that a very strong change in the fraction of long jumps, like the one found in Pd/W(211), should happen at T around half of the Debye temperature T_D of the substrate, whereas the behavior at higher T should be much smoother.

Here we consider the T dependence of the fraction of long jumps in the case of Cu, where the statistics is richer. From Table III it can be seen that the fraction of long jumps increases from 1.2% at 300 K to about 14% at 600 K. The increase is evident but not very pronounced (a dramatic increase is not expected because we are above T_D). However, if we fit the T dependence of the percentage of long jumps by a 1D Langevin model keeping the friction η constant, as done for example in Ref. 28, we obtain a smaller increase than the one found in the simulations.

C. Cross-channel mobility and correlated events

From the static energy barriers in the first column of Table II, one may predict that cross-channel mobility (always by exchange, cross-channel jumps being extremely unfavorable from the energetic point of view) would be easy in Cu, more difficult in Ag, and very difficult in Au. These results are confirmed by the results of the high-T simulations

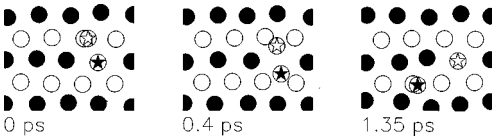

FIG. 10. Exchange-jump process in a simulation of Cu at 450 K. The adatom (open star) exchanges with one atom of the row (black star). The latter does not stop in the nearest cell in the channel but keeps moving to a further cell.

(see Table IV). In the three metals, the exchange process happens via a slightly metastable configuration at the saddle point, the so-called dumbbell configuration, in which the two atoms involved in the process are placed symmetrically along the [001] direction. This configuration was already found in many simulations of different systems.[36]

However, for what concerns cross-channel mobility, what is more interesting is the occurrence of correlated processes, such as jump-exchange (je), exchange-jump (ej), and exchange-exchange (ee) events. In Figs. 10, 11, and 12, examples of the above processes are presented. We discriminate correlated processes by requiring that the whole duration does not exceed a time of ~ 2 ps, as happens in the examples reported in the figures.

We remark that in the je and ej processes the adatoms pass again through the dumbbell configuration, as happens in the simple exchange. In the ee process, first, a strained row of three atoms along the [001] direction is created, and then the strain is released when one atom is pushed into the channel.

Those events were already observed in simulations of diffusion of Ag/Ag(110).[29] Here we compare the behavior of the three metals with this respect at $T=450$ K and analyze the behavior with T in Cu.

In Table IV, Cu, Ag, and Au are compared at 450 K. At this temperature, correlated ej and je processes are absent in Au and already rather frequent in Cu. This fact suggests that two factors favor the occurrence of these processes: first, the cross-channel-exchange barrier should be small; second, the probability of long jumps in the in-channel direction should be large. Both things happen in Cu. In fact, a je process can be described as follows as an attempt of making a double jump with a deviation in the orthogonal direction. In a typical je process, the adatom starts from the first cell, crosses a first saddle point and then the first-neighbor cell. When the adatom is reaching the second saddle point, it can be pulled or pushed by one of the nearby atoms of the close-packed rows, deviating along the [001] direction. This process is clearly more frequent if double jumps are likely to happen and if the activation energy for exchange is not large, and it is helped by the occurrence of strong lateral vibrations of the row atoms along the [001] direction.

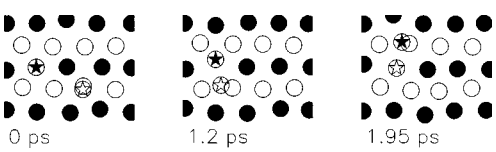

FIG. 11. Jump-exchange process in a simulation of Cu at 450 K. The adatom (open star) makes a jumps and without stopping in the nearest cell, exchanges with a row atom (black star).

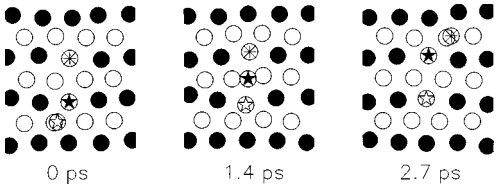

FIG. 12. Exchange-exchange process in a simulation of Cu at 450 K. The adatom (open star) pushes one of the nearest-row atoms (the black star), which in turn pushes another row atom (the asterisk). In the intermediate configuration (whose lifetime is extremely short) the three atoms are practically on a straight line along the [001] direction.

The above picture is confirmed by considering the temperature dependence of the frequency of correlated processes between 300 and 600 K in Cu (see Table III). At low temperatures, the frequency of correlated events follows the frequency of double jumps, being about one half of the latter. At the highest temperature, the frequency of correlated events increases sharply with respect to those of other events, and this is due to the enhancement of the row lateral vibrations. It is worth noting that at the highest temperature, correlated events have a very important role in cross-channel mobility: indeed 35% of the cross-channel events are correlated.

V. CONCLUSIONS

In this paper the self-diffusion of adatoms on noble-metal surfaces has been studied by molecular-dynamics simulations. The static diffusion barriers for the different processes have been calculated by quenched molecular dynamics for both (110) and (100) geometries, obtaining a good agreement with the available experimental data and calculations. A large number of high-temperature simulations have been performed for the three metals on the $(110)(1\times 1)$ surface.

The three metals display quite different diffusive behaviors. Both in-channel and cross-channel diffusion are easier in Cu than in the other metals; cross-channel diffusion is especially difficult in Au. For what concerns in-channel diffusion, the occurrence of long jumps has been analyzed in detail. Long jumps are practically absent in Au and quite frequent in Cu, Ag having an intermediate behavior. This difference comes out from two factors: first, in Au the dissipation of the energy of the adatom to the substrate is larger than in Cu and Ag; second, and more important, the potential-energy surface at the saddle point is very narrow in Au and wide in Cu. These results show the sensitivity of long jumps to the details of the interaction between the adatom and the substrate, and suggest that the use of one-dimensional models of diffusion may be insufficient also on fcc(110) metal surfaces. The sensitivity to the details of the adatom-substrate interaction may indicate an explanation of the experimental results[11] showing the absence of general trends for the occurrence of long jumps in metal-on-metal diffusion[11,13,14] (see the Introduction).

Another important difference among the three metals comes from correlated cross-channel processes. Again, we find that they are more frequent in Cu than in Ag, and absent in Au. These correlated processes are likely when there is a

significant probability of making long jumps and when the energy barrier for cross-channel diffusion is not large. Moreover, their frequency rises strongly at high temperatures, when the amplitude of the lateral vibrations of the row atoms becomes large.

Another important point that has been discussed in detail is the temperature dependence of the jump rate, in order to discuss the existence of deviations from the simple exponential behavior of the standard Arrhenius law. To this purpose, we have performed a huge number of simulations for Cu at eight different temperatures in the range 300–600 K. We have found that it is not possible to obtain a good fit of our data by a simple Arrhenius form with temperature-independent activation energy and prefactor in the whole temperature range of the simulation. However, the fit restricted to the lowest temperatures, up to 400 K, is excellent, and the estimated activation barrier is very close to the static energy barrier calculated from quenching. On the other hand, the fit restricted to the highest temperatures gives a lower activation energy and a smaller prefactor. We interpreted this activation energy reduction as caused by finite-barrier effects and, possibly, by lattice dynamics influence on diffusion.

ACKNOWLEDGMENTS

We acknowledge financial support from the Italian Ministero della Università e Ricerca under the project ''Delle superfici ideali a quelle reali.''

*Electronic address: montalenti@fisica.unige.it
†Corresponding author. Electronic address: ferrando@fisica.unige.it

[1] R. Gomer, Rep. Prog. Phys. **53**, 917 (1990).
[2] G. L. Kellogg, Surf. Sci. Rep. **21**, 1 (1994).
[3] D. W. Bassett and P. R. Webber, Surf. Sci. **70**, 520 (1978); R. T. Tung and W. R. Graham, *ibid.* **97**, 73 (1980).
[4] T. Halicioglu and G. M. Pound, Thin Solid Films **57**, 241 (1979).
[5] J. D. Wrigley and G. Ehrlich, Phys. Rev. Lett. **44**, 661 (1980).
[6] G. De Lorenzi and G. Jacucci, Surf. Sci. **164**, 526 (1985).
[7] G. L. Kellogg and P. J. Feibelman, Phys. Rev. Lett. **64**, 3143 (1990); C. L. Chen and T. T. Tsong, *ibid.* **64**, 3147 (1990).
[8] J. E. Black and Z. J. Tian, Phys. Rev. Lett. **71**, 2445 (1993).
[9] G. A. Evangelakis and N. I. Papanicolaou, Surf. Sci. **347**, 376 (1996); G. C. Kallinteris, G. A. Evangelakis, and N. I. Papanicolaou, *ibid.* **369**, 185 (1996).
[10] J. M. Cohen, Surf. Sci. **306**, L545 (1994).
[11] S. C. Wang, J. D. Wrigley, and G. Ehrlich, J. Chem. Phys. **91**, 5087 (1989); M. Lovisa and G. Ehrlich, J. Phys. (Paris), Colloq. **50**, C8-279 (1989); G. Ehrlich, Surf. Sci. **246**, 1 (1991).
[12] J. Ellis and J. P. Toennies, Phys. Rev. Lett. **70**, 2118 (1993).
[13] D. Cowell Senft and G. Ehrlich, Phys. Rev. Lett. **74**, 294 (1995).
[14] T. R. Linderoth, S. Horch, E. Laegsgaard, I. Stensgaard, and F. Besenbacher, Phys. Rev. Lett. **78**, 4978 (1997).
[15] R. Ferrando, R. Spadacini, and G. E. Tommei, Phys. Rev. E **48**, 2437 (1993).
[16] R. Ferrando, R. Spadacini, and G. E. Tommei, Surf. Sci. **265**, 273 (1992).
[17] R. Ferrando, R. Spadacini, G. E. Tommei, and G. Caratti, Surf. Sci. **311**, 411 (1994).
[18] L. Y. Chen and S. C. Ying, Phys. Rev. Lett. **71**, 4361 (1993); L. Y. Chen, M. R. Baldan, and S. C. Ying, Phys. Rev. B **54**, 8856 (1996).
[19] Yu. Georgievskii and E. Pollak, Phys. Rev. E **49**, 5098 (1994).
[20] J. Jacobsen, K. W. Jacobsen, and J. P. Sethna, Phys. Rev. Lett. **79**, 2843 (1997).
[21] S. Yu. Krylov, and A. S. Prosyanov, and J. J. M. Beenhakker, J. Chem. Phys. **107**, 6970 (1997).
[22] M. Azzouz, H. J. Kreuzer, and M. R. A. Shegelski, Phys. Rev. Lett. **80**, 1477 (1998).
[23] J. J. M. Beenhakker and S. Yu. Krylov, Surf. Sci. **411**, L816 (1998).
[24] G. De Lorenzi, G. Jacucci, and V. Pontikis, Surf. Sci. **116**, 391 (1982).
[25] J. C. Tully, G. H. Gilmer, and M. Shugard, J. Chem. Phys. **71**, 1630 (1979); A. F. Voter and J. D. Doll, *ibid.* **82**, 80 (1985).
[26] K. D. Dobbs and D. J. Doren, J. Chem. Phys. **97**, 3722 (1992).
[27] D. E. Sanders and A. E. DePristo, Surf. Sci. **264**, L169 (1992).
[28] R. Ferrando and G. Tréglia, Phys. Rev. B **50**, 12 104 (1994).
[29] R. Ferrando, Phys. Rev. Lett. **76**, 4195 (1996).
[30] G. Boisvert and L. J. Lewis, Phys. Rev. B **54**, 2880 (1996).
[31] F. Montalenti and R. Ferrando, Phys. Rev. B **58**, 3617 (1998); Surf. Sci. (to be published).
[32] V. Rosato, M. Guillopé, and B. Legrand, Philos. Mag. A **59**, 321 (1989).
[33] M. Guillopé and B. Legrand, Surf. Sci. **215**, 577 (1989).
[34] O. S. Trushin, M. Kotrla, and F. Maca, Surf. Sci. **389**, 55 (1997).
[35] K. D. Shiang, C. M. Wei, and T. T. Tsong, Surf. Sci. **301**, 137 (1994).
[36] C. J. Liu, J. M. Cohen, J. B. Adams, and A. F. Voter, Surf. Sci. **253**, 334 (1991).
[37] L. S. Perkins and A. E. DePristo, Surf. Sci. **317**, L1152 (1994).
[38] R. P. Gupta, Phys. Rev. B **23**, 6265 (1981).
[39] For a detailed discussion, see F. Ercolessi, Ph.D. thesis, ISAS, Trieste, 1987.
[40] K. W. Jacobsen, J. K. Nørskov, and M. J. Puska, Phys. Rev. B **35**, 7423 (1987).
[41] F. Ercolessi, M. Parrinello, and E. Tosatti, Philos. Mag. A **58**, 213 (1988).
[42] M. S. Daw and M. I. Baskes, Phys. Rev. Lett. **50**, 1285 (1983); Phys. Rev. B **29**, 6443 (1984).
[43] A. P. Sutton and J. Chen, Philos. Mag. Lett. **61**, 139 (1990); B. D. Todd and R. M. Lynden-Bell, Surf. Sci. **281**, 191 (1993).
[44] J. Friedel, in *Physics of Metals*, edited by J. Ziman (Pergamon, London, 1969), Vol. I.
[45] F. Ducastelle, J. Phys. Colloq. **31**, 1055 (1970).
[46] D. Tomanek, A. A. Aligia, and C. A. Balseiro, Phys. Rev. B **32**, 5051 (1985).
[47] B. Legrand and M. Guillopé, in *Atomistic Simulation of Materials*, edited by V. Vitek and D. J. Srolovitz (Plenum, New York, 1989), p. 361.
[48] C.H. Bennett, in *Diffusion in Solids, Recent Developments*, edited by A. S. Nowick and J. J. Burton (Academic, New York, 1975), p. 73.
[49] F. Hontinfinde, R. Ferrando, and A. C. Levi, Surf. Sci. **366**, 306 (1996).
[50] S. Gunther, A. Hitzke, and R. J. Behm, Surf. Rev. Lett. **4**, 1103 (1997).
[51] J. Merikoski, I. Vattulainen, J. Heinonen, and T. Ala-Nissila,

Surf. Sci. **387**, 167 (1997); J. Merikoski and T. Ala-Nissila, Phys. Rev. B **52**, 8715 (1995).
[52] P. Stolze, J. Phys.: Condens. Matter **6**, 9495 (1994).
[53] L. S. Perkins and A. E. DePristo, Surf. Sci. **294**, 67 (1993).
[54] R. C. Nelson, T. L. Einstein, S. V. Khare, and P. J. Rous, Surf. Sci. **295**, 462 (1993).
[55] M. Karimi, T. Tomkowski, G. Vidali, and O. Biham, Phys. Rev. B **52**, 5364 (1995).
[56] G. Boisvert and L. J. Lewis, Phys. Rev. B **56**, 7643 (1997).
[57] B. D. Yu and M. Scheffler, Phys. Rev. Lett. **77**, 1095 (1996); P. Ruggerone, C. Ratsch, and M. Scheffler, in *Growth and Properties of Ultrathin Epitaxial Layers*, edited by D. A. King and D. P. Woodruff (Elsevier, Amsterdam, 1997).
[58] B. D. Yu and M. Scheffler, Phys. Rev. B **56**, 15 569 (1997).
[59] M. Breeman and D. O. Boerma, Surf. Sci. **269-170**, 224 (1992).
[60] H. Durr, J. F. Wendelken, and J.-K. Zuo, Surf. Sci. **328**, L527 (1995).
[61] J. J. de Miguel, A. Sanchez, A. Cebollada, J. M. Gallego, J. Ferron, and S. Ferrer, Surf. Sci. **189/190**, 1062 (1987).
[62] H. J. Ernst, F. Fabre, and J. Lapujoulade, Phys. Rev. B **46**, 1929 (1992).
[63] M. H. Langelaar, M. Breeman, and D. O. Boerma, Surf. Sci. **352-354**, 597 (1996).
[64] L. Bardotti, M. C. Bartelt, C. J. Jenks, C. R. Stoldt, J.-M. Wen, C.-M. Zhang, P. A. Thiel, and J. W. Evans, Langmuir **14**, 1487 (1998).
[65] L. D. Roelofs, J. I. Martin, and R. Sheth, Surf. Sci. **250**, 17 (1991).
[66] L. Hansen, P. Stoltze, K. W. Jacobsen, and J. K. Nørskov, Phys. Rev. B **44**, 6523 (1991).
[67] T. S. Rahman and Z. J. Tian, J. Electron Spectrosc. Relat. Phenom. **64/65**, 651 (1993).
[68] M. P. Allen and D. J. Tildesley *Computer Simulation of Liquids* (Clarendon, Oxford, 1987).
[69] U. Kürpick, A. Kara, and T. S. Rahman, Phys. Rev. Lett. **78**, 1086 (1997); **80**, 204 (1998).
[70] U. Kürpick and T. S. Rahman, Surf. Sci. **383**, 137 (1997).
[71] G. Boisvert, N. Mousseau, and L. J. Lewis, Phys. Rev. Lett. **80**, 203 (1998).
[72] G. Boisvert, N. Mousseau, and L.J. Lewis, Phys. Rev. B **58**, 12 667 (1998).
[73] G. A. Evangelakis, D. G. Papageorgiou, G. K. Kallinteris, Ch. E. Lekka, and N. I. Papanicolaou, Vacuum **50**, 165 (1998).
[74] R. Ferrando and G. Trëglia, Phys. Rev. Lett. **76**, 2109 (1996).
[75] D. E. Sanders and A. E. DePristo, Surf. Sci. **260**, 116 (1992).
[76] G. A. Evangelakis, G. C. Kallinteris, and N. I. Papanicolaou, Surf. Sci. **394**, 185 (1997).
[77] G. Boisvert, N. Mosseau, and L. J. Lewis, Phys. Rev. Lett. **80**, 203 (1998).
[78] G. Caratti, R. Ferrando, R. Spadacini, and G. E. Tommei, Phys. Rev. E **54**, 4708 (1996).
[79] V. P. Zhdanov, Surf. Sci. **214**, 289 (1989).
[80] L. D. Roelofs, B. J. Greenblatt, and N. Boothe, Surf. Sci. **334**, 248 (1995).
[81] T. Ala-Nissila and S. C. Ying, Prog. Surf. Sci. **39**, 227 (1992).
[82] H. Risken, *The Fokker-Planck Equation* (Springer, Berlin, 1989).
[83] S. C. Ying, Phys. Rev. B **41**, 7068 (1990).
[84] J. R. Banavar, M. H. Cohen, and R. Gomer, Surf. Sci. **107**, 113 (1981).
[85] G. Caratti, R. Ferrando, R. Spadacini, and G. E. Tommei, Chem. Phys. **234**, 157 (1998); Phys. Rev. E **55**, 4810 (1997).
[86] V. I. Mel'nikov, Phys. Rep. **209**, 1 (1991).